

# The Characterization of Nylon 6 Filaments by X-Ray Diffraction

R. F. STEPANIAK, A. GARTON, D. J. CARLSSON, and D. M. WILES,  
*Division of Chemistry, National Research Council of Canada, Ottawa,  
Ontario K1A 0R6, Canada*

## Synopsis

A method is described for calculating crystallinity indices and crystalline orientation functions for the  $\alpha$  and  $\gamma$  components of the crystalline phase of nylon 6 filaments using wide-angle x-ray diffraction (WAXS) analysis. The method is shown to be applicable to a wide range of filament samples ("conventional" as-spun, fast spun, drawn, and annealed) even when only a single broad diffraction maximum is observable from the WAXS photograph. The component indices can be used to illustrate differences present in the filament microstructure which would be unobservable if a total crystallinity index, such as that determined by density, were determined alone. For example, the initially mixed  $\alpha$ - $\gamma$  structure is retained in low-temperature drawing (75–150°C) of nylon 6 fiber, but the predominantly  $\alpha$  form is produced at higher draw temperatures.

## INTRODUCTION

Fabrication conditions for thermoplastic fiber-forming polymers determine the physical and, to a certain extent, chemical behavior of the resultant fibers. Thus, the potential usefulness of synthetic fibers such as polyamides can be optimized by appropriate control at the extrusion, orienting, and annealing stages. It is important, therefore, to be able to quantitatively relate the microstructure of semicrystalline polymers to their production history by techniques such as x-ray diffraction analysis.

The literature concerning the quantitative analysis of nylon 6 by wide-angle x-ray diffraction (WAXS) is fragmented and often contradictory. In part, this has resulted from disagreements concerning the nature and nomenclature of the different crystalline forms present. This aspect of the problem has recently been reviewed by Parker and Lindenmeyer.<sup>1</sup> A reasonable rationalization is that there exist only two basic crystallographic forms,  $\alpha$  and  $\gamma$ .<sup>2-4</sup>

Nylon 6 in the pseudo-hexagonal  $\gamma$  form is produced when the melt is rapidly quenched,<sup>2</sup> and this may be converted into the monoclinic<sup>5</sup>  $\alpha$  form by annealing or drawing. An oriented  $\gamma$  form can be produced directly by melt spinning at high speeds.<sup>2</sup> The  $\gamma$  form may also be generated by immersion of the  $\alpha$  form in a solution of iodine in aqueous potassium iodide.<sup>6,7</sup> Both the fast-spun and iodine-treated  $\gamma$  forms cannot, however, be reconverted to the  $\alpha$  form by a conventional annealing step.<sup>1,7</sup>

Attempts to obtain a measure of the relative amounts of  $\alpha$ ,  $\gamma$ , and amorphous nylon 6 present in a given sample have met with only limited success. Implicit in the method of Roldan et al.<sup>8</sup> is the assumption of the existence of a separate  $\beta$  phase. The calculations of Kyotani and Mitsuhashi<sup>9</sup> rely on peak heights and not integrated peak intensities and so will be greatly influenced by crystallite

size and perfection. The crystallization perfection index of Dismore and Statton,<sup>10</sup> originally employed for nylon 66, could be applied to nylon 6 and would involve a calculation of the separation of the (200) and (002,202) maxima and is therefore limited to samples where resolvable maxima exist (i.e., fairly well-developed  $\alpha$  structures). Perhaps the most successful treatment thus far is the mathematical model developed by Huisman, Heuvel, and Lind.<sup>3</sup> Three curves, assumed to be representative of the  $\alpha$  and  $\gamma$  equatorial diffraction, are fitted by computer to the observed equatorial diffractometer scans. A major limitation of the method is that the  $\gamma$  and amorphous contributions had to be treated together as one of the three curves.

A second important morphological characteristic of fiber samples is crystalline orientation. The absence of suitable meridional reflections in the monoclinic  $\alpha$  form of nylon 6 makes the estimation of crystalline orientation difficult. Dumbleton et al.<sup>11</sup> used the (1 14 3) reflection of nylon 66 which occurs at  $2\theta = 77^\circ$  and assumed it to be coincident with the chain axis (an error of  $\sim 2^\circ$ ). In this way approximate values of the Hermans-Stein crystalline orientation functions ( $f$ ) were calculated for hot-drawn nylon 66 samples. In principle, a similar approach would be possible for nylon 6. Alternatively,  $f_a$  and  $f_c$  may be calculated for nylon 6 from the (200) and (002,202) reflections of the  $\alpha$  form and  $f_b$  (corresponding to the orientation of the crystalline chains) calculated assuming the unit cell to be orthogonal and not monoclinic.<sup>12</sup> Sakaoku, Morosoff, and Peterlin<sup>13</sup> reported orientation functions for drawn then annealed (highly  $\alpha$ ) samples using a Wilchinsky<sup>14</sup> formula but did not give details of the assumptions involved. Alternatively, a semiquantitative index of orientation may be obtained using the width at half-height of the azimuthal intensity distribution of a selected reflection.<sup>15</sup> The orientation of as-spun filaments has been calculated by assuming that the sample was completely in the pseudohexagonal  $\gamma$  form and further assuming true hexagonal symmetry for this structure.<sup>2</sup>

We describe here empirical methods for calculating a total crystalline index, crystalline indices for the  $\alpha$  and  $\gamma$  forms, and the corresponding  $\alpha$  and  $\gamma$  orientation functions for any sample of nylon 6. Although several assumptions are necessary, these are kept to a minimum, and some of the limitations of earlier methods are avoided. Using these techniques a variety of nylon 6 filaments (conventional as spun, fast spun, drawn, and annealed) are quantitatively characterized. Corresponding density and some infrared (IR) spectroscopy measurements are also reported.

## EXPERIMENTAL

Nylon 6 tapes and filaments were prepared in our laboratories using a modified Maxwell-type extruder<sup>16</sup> and fiber-grade resin supplied by Dow-Badische Ltd., Arnprior, Ontario. The pellets were vacuum dried before use. Cooling of the extrudate took place by passage through still air. The temperature of the melt at the spinneret was about  $250^\circ\text{C}$  and take-up speeds were typically 20 m/min to produce low orientation monofilaments ( $\sim 200\ \mu\text{m}$  diameter) and 3000 m/min (with a higher extruder throughput) to produce highly oriented ( $\sim 25\ \mu\text{m}$  diameter) "fast spun" filaments. Samples were either rapidly removed from the take-up device and stored in a vacuum desiccator ("dry" samples) or were stored under controlled conditions ( $23^\circ\text{C}$ , 65% relative humidity). No spin finish or other lubricant was used during the fiber production process.

Off-line drawing took place through a 50-cm air oven at several different temperatures. Long oven residence times were used (~12 sec) to allow the filaments to reach the oven temperature. The draw ratio was calculated from the ratio of the speeds of the feed and the take-up rollers. Annealing took place under vacuum (to reduce degradation) with the samples wound tightly around a bobbin. The annealing time was kept constant at 150 min.

WAXS patterns were obtained using  $\text{CuK}\alpha$  radiation from a conventional Philips generator and a commercially available x-ray camera designed by Statton.<sup>17</sup> For the calculation of crystallinity indices a rotated sample was used to eliminate orientation effects. The sample-to-film distance was usually 50 mm. The resulting photographs were analyzed with a Joyce-Loebl scanning microdensitometer. To calculate orientation functions, radial densitometer scans were performed on the diffraction pattern of a stationary sample every  $2.5^\circ$  over one quadrant.

Filament densities were obtained using a carbon tetrachloride/hexane density gradient column at  $23^\circ\text{C}$ . Infrared spectra of tapes and filaments were obtained using a Beckman 4210 grating spectrometer. The very low IR transmission of single filaments and small filament bundles necessitated the use of a special sample holder and a wide slit setting on the spectrometer.<sup>18</sup>

### ANALYSIS OF WAXS DATA

Calculation of crystalline indices from the diffraction pattern of a rotated sample involves first a linear background correction and then the subtraction of an amorphous component. An amorphous "template" was obtained by examining the azimuthal intensity distribution of a highly oriented sample. A radial densitometer scan at the azimuth of minimum intensity was used to calculate the amorphous template. This basic amorphous peak was observed to be essentially constant in position and shape from sample to sample. The amorphous template was scaled such that it best superimposed the intensity observed in a radial densitometer scan of a rotated sample in the region  $2\theta = 14.0\text{--}18.0^\circ$  (Fig. 1). A total crystalline contribution was then readily obtained by subtracting the amorphous intensity from the overall intensity.

Indices which describe the relative amounts of the crystalline component in the  $\alpha$  and  $\gamma$  forms can be readily determined by invoking the assumption that all specimens of partially crystalline nylon 6 contain varying amounts of the  $\alpha$  and  $\gamma$  structures. The (200) and (202,002) reflections of the  $\alpha$  form were assumed to occur at  $2\theta = 20.0^\circ$  and  $2\theta = 24.0^\circ$ , respectively. These values of the Bragg angle were obtained from the positions of the reflections in a highly annealed ( $205^\circ\text{C}$ ) sample with very high  $\alpha$  crystalline content. Furthermore, all crystalline scattering intensity in the region  $2\theta = 18.0\text{--}20.0^\circ$  and to the high-angle side of  $2\theta = 24.0^\circ$  was considered to result from the  $\alpha$  structure. These intensity regions were also assumed to be symmetrically distributed as in a highly  $\alpha$  sample. Thus, in Figure 1, the relative proportion of  $\alpha$  scattering is  $2a + 2c$ , whereas the  $\gamma$  scattering is taken to be  $I_{020} + b - a - c$ .  $I_{020}$  ( $2\theta = 9\text{--}13^\circ$ ) is assigned wholly to the  $\gamma$  structure since the intensity of this reflection in the  $\alpha$  phase is very low.<sup>5</sup>

The total crystalline index as well as the  $\alpha$  and  $\gamma$  indices are expressed as a fraction of the total scatter. These manipulations were readily performed nu-

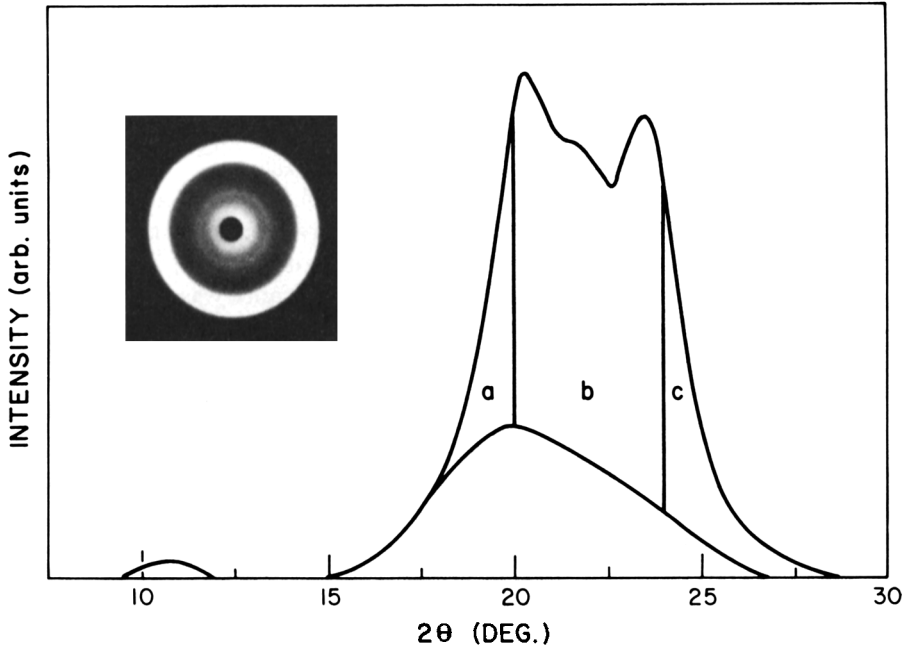


Fig. 1. Analysis of WAXS data. As-spun filament annealed at 180°C.

merically using a PDP-8 (32K core) computer or graphically with the aid of a du Pont 610 curve resolver.

Orientations of the monoclinic  $\alpha$  phase may be calculated from the equation of Wilchinsky<sup>14</sup> using the crystallographic data of Holmes, Bunn, and Smith.<sup>5</sup> In such a way we obtained the relation

$$\langle \cos^2 \phi_{b,z} \rangle = 1.0 - 1.204 \langle \cos^2 \phi_{200,z} \rangle + 6.556 \langle \cos^2 \phi_{202,z} \rangle - 7.351 \langle \cos^2 \phi_{002,z} \rangle \quad (1)$$

where  $\phi_{hkl,z}$  is the angle made by the  $hkl$  plane normal to the  $z$ -axis (fiber axis) and  $\phi_{b,z}$  is the angle made by the crystallographic  $b$ -axis to the  $z$ -axis. The  $b$ -axis is chosen to be coincident with the crystal chain axis. Since the (002) and the (202) reflections overlap for  $\alpha$  nylon 6, we must assume that

$$\langle \cos^2 \phi_{002,z} \rangle = \langle \cos^2 \phi_{202,z} \rangle \quad (2)$$

Thus

$$\langle \cos^2 \phi_{b,z} \rangle = 1.0 - 1.204 \langle \cos^2 \phi_{200,z} \rangle - 0.795 \langle \cos^2 \phi_{202,z}^{002} \rangle \quad (3)$$

Hermans-Stein orientation functions<sup>17</sup> may be defined as

$$f_a = \frac{3}{2} \langle \cos^2 \phi_{200,z} \rangle - \frac{1}{2}$$

$$f_c = \frac{3}{2} \langle \cos^2 \phi_{202,z}^{002} \rangle - \frac{1}{2}$$

$$f_b = \frac{3}{2} \langle \cos^2 \phi_{b,z} \rangle - \frac{1}{2}$$

The orientation functions of the  $\gamma$  form were calculated by assuming true hexagonal symmetry. The Hermans-Stein orientation functions may be calculated from the equatorial reflection, and the Wilchinsky relation<sup>2</sup>

$$2f_a = 2f_b = -f_c$$

may be used to calculate  $f_c$  ( $c$  = chain axis).

Integrated peak intensities for the (200) and (002,202) reflections of the  $\alpha$  form and for the (002) reflection of the  $\gamma$  form were obtained as a function of azimuthal angle in the range  $\rho = 0-90^\circ$  from radial densitometer scans performed every  $2.5^\circ$ . Each scan was analyzed for  $\alpha$  and  $\gamma$  components (cf. Fig. 1). The derived intensities were then expressed as a function of  $\phi$  using the geometric relationship

$$\cos \phi = \cos \theta \cos \rho$$

and used to obtain orientation functions for the  $\alpha$  and  $\gamma$  components.

The  $\langle \cos^2 \phi_{hkl,z} \rangle$  value was obtained from the integral

$$\langle \cos^2 \phi_{hkl,z} \rangle = \frac{\int_0^{\pi/2} I(\phi) \sin \phi \cos^2 \phi \, d\phi}{\int_0^{\pi/2} I(\phi) \sin \phi \, d\phi}$$

The integrations were performed numerically on a computer using data points at  $2.5^\circ$  intervals. Intensity data for  $\phi = 0-\theta$  were not obtainable from flat plate photographs, and so  $I(\phi)$  in this angular range was set equal to  $I(\theta)$ .

## RESULTS

### Characterization of As-Spun Filaments

Crystallinity indices for conventional and fast spun filaments were calculated as described above and are shown in Table I. Also presented in Table I are the density data and the  $\gamma$  component orientation functions of the faster-spun filaments. WAXS patterns from stationary samples and radial densitometer scans from rotated samples are shown in Figure 2. Both samples were conditioned at  $23^\circ\text{C}$  and 65% R.H. for more than one week before examination, since it has been demonstrated that crystallization generally occurs during storage of the fiber on the bobbin and not on the spinline as is the case for polyolefins.<sup>2</sup> The sample spun at very slow speed (Table I) exhibits approximately equal amounts of  $\alpha$  and  $\gamma$  components. Increasing take-up speed is shown to be associated with

TABLE I  
Characterization of As-Spun Filaments

Filament take-up rate, m/min	Crystalline index	$\alpha$ Index	$\gamma$ Index	Density, g/cm <sup>3</sup>	$\gamma$ Orientation	
					$f_a/f_b$	$f_c$
20 (conventional)	50	23	27	1.1204	—	—
500	52	23	29	1.1260	-0.16	0.33
1130	57	24	33	1.1315	-0.34	0.68
1980	58	20	39	—	—	—
2435	63	22	42	1.1348	-0.37	0.73

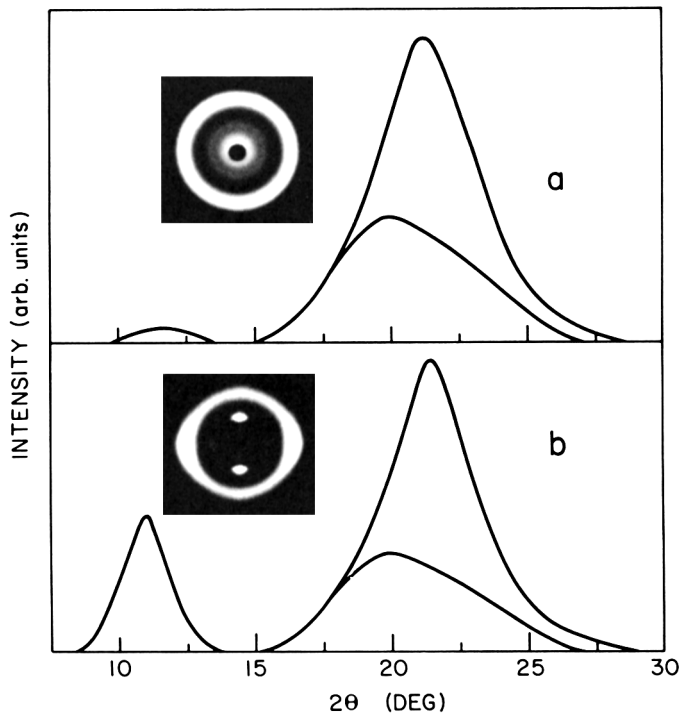


Fig. 2. Radial densitometer scan (background removed) from rotated as-spun filaments. Stationary WAXS photographs inset: (a) take-up speed 20 m/min; (b) Take-up speed 2435 m/min.

increases in total crystalline index,  $\gamma$  component index, and orientation, while the  $\alpha$  component index remains approximately constant.

### Annealing of Conventional As-Spun Filaments

The crystalline transformations that occurred on annealing were examined using WAXS, density, and IR spectroscopic measurements. The total crystallinity index and the density were shown to increase in a similar manner with increasing annealing temperature (Fig. 3). Unlike the density determinations, however, WAXS analysis allows separation of the two components of the crystalline phase (Fig. 4). At low annealing temperatures ( $<130^{\circ}\text{C}$ ), both the  $\alpha$  and  $\gamma$  indices marginally increase with increasing temperature; at  $>130^{\circ}\text{C}$ , the  $\alpha$  index increases rapidly whereas the  $\gamma$  index decreases.

IR measurements showed similar trends for these samples. The as-spun sample exhibited a broad absorption in the  $690\text{--}720\text{ cm}^{-1}$  range characteristic of a superposition of  $\alpha$  ( $692\text{ cm}^{-1}$ ) and  $\gamma$  ( $708\text{ cm}^{-1}$ ) absorptions.<sup>18</sup> The  $205^{\circ}\text{C}$  annealed sample had a much sharper absorption centered at about  $695\text{ cm}^{-1}$  together with an absorption at  $928\text{ cm}^{-1}$  characteristic of the  $\alpha$  form.<sup>6</sup>

Stress-strain curves of annealed samples were also examined. The yield stresses were found to be approximately constant ( $\sim 2.5 \times 10^8\text{ dynes/cm}^2$ ) for annealing temperatures less than  $100^{\circ}\text{C}$ . At higher temperatures yield stresses increased linearly to a value of  $4.8 \times 10^8\text{ dynes/cm}^2$  for annealing at  $205^{\circ}\text{C}$ . Fiber tensile strength decreased significantly for samples annealed at high temperatures ( $>150^{\circ}\text{C}$ ).

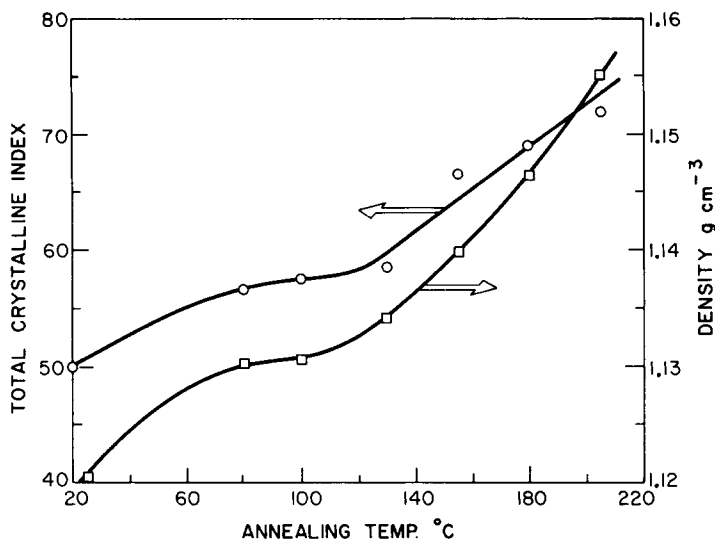


Fig. 3. Annealing of as-spun filament under vacuum (150 min).

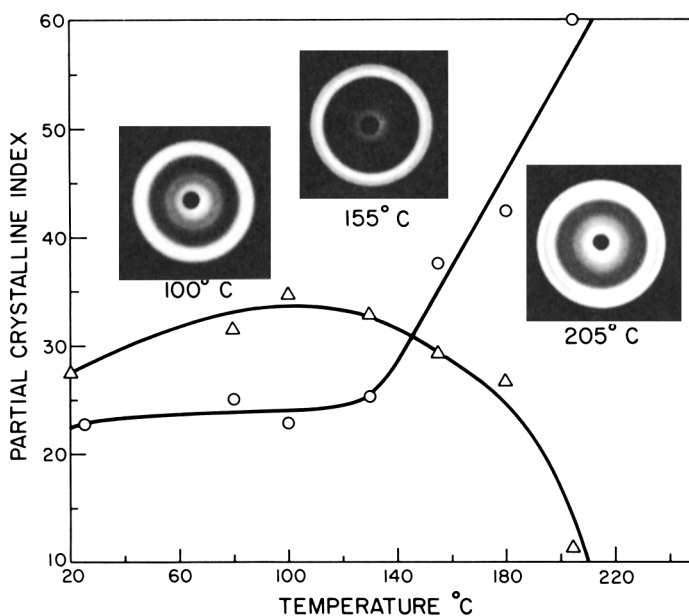


Fig. 4. Annealing of as-spun filament under vacuum: (○) α crystalline index; (Δ) γ crystalline index.

### Drawing of Conventional As-Spun Filaments

Some WAXS photographs of the as-spun filament drawn 2.3X at various temperatures (oven residence time 12 sec) are shown in Figure 5. Differences in densities and total crystallinity indices for these samples (Fig. 6) were small in comparison to those produced by annealing (Fig. 3). The response of the α and γ crystalline indices to the various draw temperatures was however much more dramatic. At high draw temperatures a predominantly α structure was produced. Quantitative IR measurements on oriented samples are difficult

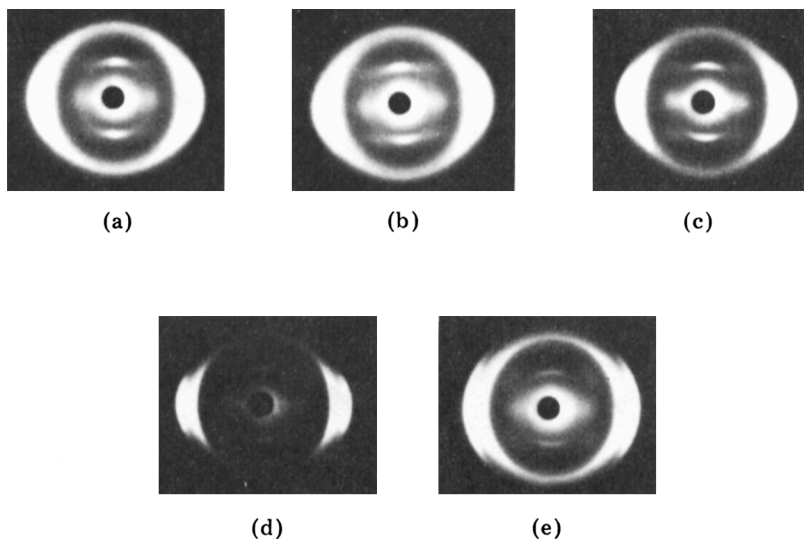


Fig. 5. As-spun filament drawn 2.3X at various temperatures: (a) 80°C; (b) 100°C; (c) 130°C; (d) 155°C; (e) 180°C.

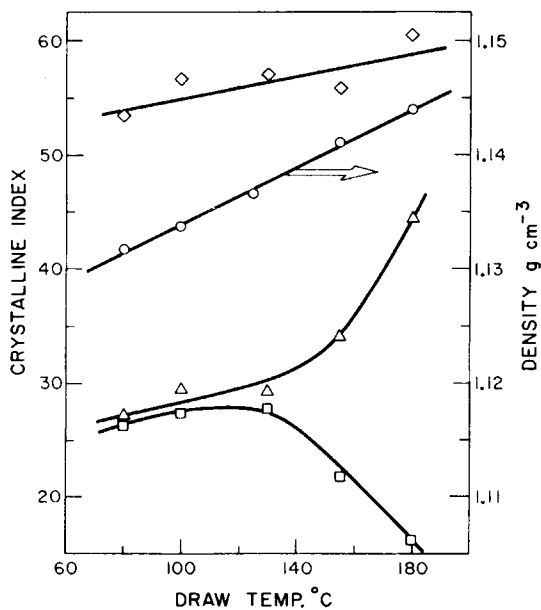


Fig. 6. As-spun filament drawn 2.3X at various temperatures: (◇) total crystalline index; (△)  $\alpha$  crystalline index; (□)  $\gamma$  crystalline index; (○) density.

because of the polarization-sensitive nature of the IR bands, but the transition from a mixed structure to a predominantly  $\alpha$  form with increasing draw temperature was confirmed by the marked increase in the intensity of the  $928\text{ cm}^{-1}$   $\alpha$  absorption band with increasing draw temperature. Higher draw ratios increased the total crystalline index and the density of the sample.

At a fixed draw temperature (180°C), crystalline orientation functions (Table II) were shown, as expected, to increase with increasing draw ratio. More in-



TABLE II  
 Orientation of Drawn Nylon 6 Filaments<sup>a</sup>

Draw temperature, °C	$\alpha$ Orientation			$\gamma$ Orientation		Density, g/cm <sup>3</sup>
	$f_a$	$f_c$	$f_b$	$f_a f_b$	$f_c$	
80	-0.24	-0.39	0.59	-0.27	0.54	1.1318
100	-0.29	-0.41	0.68	-0.32	0.64	1.1338
130	-0.32	-0.42	0.72	-0.35	0.70	1.1367
155	-0.27	-0.43	0.68	-0.36	0.72	1.1412
180	-0.21	-0.39	0.56	-0.28	0.56	1.1440
180 (×1.7)	-0.12	-0.30	0.38	-0.25	0.51	1.1444
180 (×5.0)	-0.47	-0.47	0.94	-0.48	0.95	1.1464

<sup>a</sup> Drawn 2.3× unless otherwise indicated.

formative is the observation that the  $\alpha$  and  $\gamma$  components appear to orient to a similar degree during drawing both at different temperatures and draw ratio. At a constant draw ratio of 2.3×, the crystalline orientation, under our draw conditions, maximized at a draw oven temperature of 130–155°C.

## DISCUSSION

Any calculation of percentage crystallinity implicitly involves a definition of crystallinity, and problems will clearly occur in defining defective structures such as polymer crystallites. For this reason we prefer the term crystallinity index in the present discussion. The usefulness of the approach employed in this study, however, lies in its ability to resolve the crystalline diffraction into two components for a wide range of samples, particularly those with poorly defined diffraction patterns such as as-spun or cold-drawn filaments.

The assumptions that the (200) and (202,002) reflections of the  $\alpha$  form occur at  $2\theta = 20.0^\circ$  and  $24.0^\circ$ , respectively, and that all the crystalline scatter in the range  $2\theta = 18\text{--}20^\circ$  and  $>24^\circ$  results from the  $\alpha$  form lead to the  $\alpha$  crystalline index being a measure of the "perfect"  $\alpha$  content. The  $2\theta$  values were chosen to correspond to the maxima of a highly annealed sample and agree well with those found in the  $\alpha$  structure determination.<sup>5</sup> The remainder of the crystalline scattering is included in the  $\gamma$  index, which will therefore be rather less well defined and probably includes some contribution from imperfect  $\alpha$  structures. Reconstruction of the  $\gamma$  diffraction in this way generally produces a pattern quite similar in shape and position to that of a highly developed  $\gamma$  structure (iodine/potassium iodide immersed or fast spun). This implies that little is to be gained by considering distorted  $\alpha$  and  $\gamma$  unit cells in calculating the component indices as was recommended by Parker and Lindenmeyer.<sup>1</sup>

The full quantitative description of the crystalline structure, particularly the calculation of orientation functions, is a rather laborious process using the techniques described here, although there is considerable scope for automation given adequate diffractometer and computing facilities. WAXS analysis does, however, provide a very sensitive tool for studying structural changes that occur during film and fiber production. Furthermore, combined with birefringence or sonic modulus data, a calculation of crystallinity then allows the important parameter of amorphous orientation function,  $f_{am}$ , to be calculated.<sup>20</sup>

The calculation of separate  $\alpha$  and  $\gamma$  crystallinity indices is much more infor-

mative than a total crystallinity index (calculated either from density or WAXS measurements). This is demonstrated in Figures 4 and 6 where large changes in the proportions of the two components are masked if overall crystallinity alone is considered. A similar conclusion is inferred from IR measurements, but practical difficulties, particularly with small, highly oriented samples, limit the usefulness of this technique.

Changes in the intensity of the (020) reflection also provide information about the structural state of the sample. The conventional as-spun filament (after conditioning) has approximately equal component indices (Table I) and a low-intensity (020) reflection (Fig. 2). Increasing take-up velocity increases the  $\gamma$  index but also more dramatically increases the intensity of the (020) reflection. This implies that increasing the take-up velocity increases the proportion as well as the perfection of the  $\gamma$  component. Research is continuing into the physical, chemical, and structural properties of the  $\gamma$  structures obtained by different preparative routes.

## CONCLUSIONS

The proposed method of analysis of the WAXS data has been applied to resolve the changes that occur on spinning, drawing, and annealing nylon 6 filaments. Several important conclusions may be reached.

1. Nylon 6 filaments produced at conventional spinning speeds have (after conditioning) approximately equal  $\alpha$  and  $\gamma$  crystalline indices. Increasing the take-up speed during melt spinning increases the crystalline index (Table I), the crystalline perfection (Fig. 2), and the crystalline orientation (Table I) of as-spun filaments. At very high spinning speeds a filament with tensile properties very similar to conventional hot-drawn filaments is produced (typically ~70% residual elongation). The highly oriented hot drawn filaments, however, have a predominantly  $\alpha$  crystal structure while the fast spun filament has the  $\gamma$  form, cf. WAXS patterns in Figures 2(b) and 5.

2. When conventional as-spun filaments are annealed under vacuum (i.e., low residual water content), conversion of the  $\gamma$  form to the  $\alpha$  form only occurs at  $>120^\circ\text{C}$ . At lower annealing temperatures, both the  $\alpha$  and  $\gamma$  crystalline indices increase marginally with annealing (Fig. 4).

3. Drawing of conditioned (65% R.H.) as-spun filaments results in an appreciable increase in the overall crystallinity, this effect increasing with increasing draw temperature and draw ratio. More significantly, the proportions of the  $\alpha$  and  $\gamma$  components also change with drawing. The mixed structure is retained at low draw temperatures, but a predominantly  $\alpha$  form is produced at high draw temperatures.

4. Under otherwise constant draw conditions crystalline orientation maximized at a draw oven temperature of  $130\text{--}155^\circ\text{C}$ . There is little apparent difference in the orientation levels of the two crystalline forms for all of the draw conditions employed.

## References

1. J. P. Parker and P. H. Lindenmeyer, *J. Appl. Polym. Sci.*, **21**, 821 (1977).
2. V. G. Bankar, J. E. Spruiell, and J. L. White, *J. Appl. Polym. Sci.*, **21**, 2341 (1977).
3. R. Huisman, H. M. Heuvel, and K. C. J. B. Lind, *J. Polym. Sci., Polym. Phys. Ed.*, **14**, 921 (1976); R. Huisman and H. M. Heuvel, *ibid.*, **14**, 941 (1976).

4. T. Ishibashi and T. Ishii, *J. Appl. Polym. Sci.*, **20**, 335 (1976).
5. D. R. Holmes, C. W. Bunn, and D. I. Smith, *J. Polym. Sci.*, **17**, 159 (1955).
6. H. Arimoto, *J. Polym. Sci. A*, **2**, 2283 (1964).
7. K. H. Illers, H. Haberkorn, and P. Simak, *Makromol. Chem.*, **158**, 285 (1972).
8. L. G. Roldan, R. Rahl, and A. R. Paterson, *J. Polym. Sci. C*, **8**, 145 (1965).
9. M. Kyotani and S. Mitsuhashi, *J. Polym. Sci. A-2*, **10**, 1497 (1972).
10. P. F. Dismore and W. O. Statton, *J. Polym. Sci.*, **C 13**, 133 (1966).
11. J. H. Dumbleton, D. R. Buchanan, and B. B. Bowles, *J. Appl. Polym. Sci.*, **12**, 2067 (1968).
12. K. Inoue and S. Hoshino, *J. Polym. Sci., Polym. Phys. Ed.*, **15**, 1363 (1977).
13. K. Sakaoku, N. Morosoff, and A. Peterlin, *J. Polym. Sci., Polym. Phys. Ed.*, **11**, 31 (1973).
14. Z. W. Wilchinsky, *Advances in X-Ray Analysis*, Vol. 6, Plenum, New York, 1963, p. 231.
15. D. C. Prevorsek, P. J. Harget, R. K. Sharma, and A. C. Reimschuessel, *J. Macromol. Sci., Phys.*, **B8**, 127 (1973).
16. D. J. Carlsson, A. Garton, and D. M. Wiles, *J. Appl. Polym. Sci.*, **21**, 2963 (1977).
17. L. E. Alexander, *X-Ray Diffraction Methods in Polymer Science*, Wiley, New York, 1964.
18. D. J. Carlsson, F. R. S. Clark, and D. M. Wiles, *Text. Res. J.*, **46**, 318 (1976).
19. I. Matsuura and J. H. Magill, *J. Polym. Sci., Polym. Phys. Ed.*, **11**, 1173 (1973).
20. R. J. Samuels, *Structured Polymer Properties*, Wiley, New York, 1974.

Received March 22, 1978

Revised April 28, 1978